Kovacs Effect Studied Using The Distinguishable Particles Lattice Model Of Glass

Matteo Lulli,[1] Ling-Han Zhang,[2] Chun-Shing Lee,[1] Hai-Yao Deng,[3] and Chi-Hang Lam[1, *]

[1]*Department of Applied Physics, Hong Kong Polytechnic University, Hong Kong, China*[†]

[2]*Department of Physics, Carnegie Mellon University, Pittsburgh, Pennsylvania 15213, USA*

[3]*School of Physics and Astronomy, The University of Manchester, Manchester M13 9PL, United Kingdom*

(Dated: October 24, 2019)

Kovacs effect is a characteristic feature of glassy relaxation. It consists in a non-monotonic evolution of the volume (or enthalpy) of a glass after a succession of two abrupt temperatures changes. The second change is performed when the instantaneous value of the volume coincides with the equilibrium one at the final temperature. While this protocol might be expected to yield equilibrium dynamics right after the second temperature change, the volume instead rises and reaches a maximum, the so-called Kovacs hump, before dropping again to the final equilibrium value. Kovacs effect constitutes one of the hallmarks of aging in glasses. In this paper we reproduce all features of the Kovacs hump by means of the Distinguishable Particles Lattice Model (DPLM) which is a particle model of structural glasses.

INTRODUCTION

Kovacs' series of experiments [1] is fundamental to our present understanding of non-equilibrium glassy dynamics [2–4] highlighting the non-linear features of aging. Kovacs [1] thoroughly analyzed the volume relaxation dynamics of polymer glasses induced by rapid temperature changes, or *temperature jumps*. Two important results are the *expansion gap paradox* [5–12] and the renowned *Kovacs effect* [13–20], for single- and double-temperature jumps respectively. The former refers to an apparent difference in the instantaneous relaxation time near equilibrium, between heating (up-jump) and cooling (down-jump), after a single temperature change is performed. On the other hand, Kovacs effect shows that the instantaneous value of the volume (or enthalpy [21, 22]) during the relaxation, is not a sufficient indicator of the departure from equilibrium of the system. After a first temperature jump from the initial temperature T_i to the annealing temperature T_a (with $T_a < T_i$), the relaxation can be interrupted when the observable reaches the equilibrium value characteristic of a third final temperature T_f by a second temperature jump from T_a to T_f (with $T_a < T_f < T_i$): One observes a non-monotonic evolution of the observable that reaches a maximum (i.e. *Kovacs hump*) before relaxing back to the already-attained equilibrium value. Most existing works have focused on reproducing the *Kovacs effect* by means of finite-dimensional and mean-field spin-glass models [13, 15, 23], ordered XY and Ising models [14, 23, 24], molecular dynamics [16], kinetically constrained models (KCMs) [17, 18] and simple two-level systems [19, 20]. Mean-field constitutive models have also been used, most notably the Tool-Narayanaswamy-Moynihan [25–27] and the Kovacs-Aklonis-Hutchinson-Ramos [28] models, as well as those accounting for spatial fluctuations of observables, such as

a stochastic version of a free-volume model [29] and the Stochastic Constitutive Model (SCM) [30].

We reproduce all the features of Kovacs effect using the recently developed Distinguishable Particles Lattice Model (DPLM) [31]. The phonon temperature, which is subjected to two consecutive jumps, is modeled by the bath temperature of the kinetic Monte Carlo simulation of the DPLM. It has been shown that the DPLM displays many features of the particles dynamics of glass formers with exactly known equilibrium properties [31, 32]. In particular, we have been able to reproduce, for the first time with a particle model, the expansion gap paradox [33], and provide an intuitive explanation in terms of a local *structural temperature* whose dynamics is spatially unstable in the up-jump case. Furthermore, the DPLM allows for a tuning of the *kinetic fragility* [32] over a very wide range of values, which can be, in principle, arbitrarily large. The relation between kinetic and thermodynamic fragility correctly captures several experimental features as well. It has also been possible to obtain an approximate analytical expression for the particle mean squared displacement [34, 35] for this model.

We observe the characteristic Kovacs hump during the system energy relaxation, analogous to enthalpy relaxation in experiments [21, 22]. This paper demonstrate the ability of the DPLM to reproduce experimental signatures of glassy systems observed in Kovacs' experiments [1]. We demonstrate that, while correctly reproducing the expansion gap [33], the DPLM is also able to capture the Kovacs effect. To the best of our knowledge only two constitutive models, namely the SCM [30] and the free-volume model [29], have been shown to reproduce both effects.

MODEL DEFINITION

We simulate the DPLM [31] defined on a 2-dimensional lattice of linear size $L = 100$ where the sites are occupied by N distinguishable particles, each of them associated to a *unique label* $s_i = 1, \ldots, N$. An important property of the model is that each particle is coupled to its nearest neighbors by means of *site-* and *labels-dependent* random interactions: Considering the interaction energy associated to the particles sitting at sites i and j, with labels s_i and s_j, one has a four-indices quantity $V_{ijs_is_j}$. In order to simulate the hopping of particles we consider the presence of $N_v = 50$ voids, i.e. given that $L^2 = N + N_v$ one has a void density $\phi_v = N_v/L^2 = 0.005$. One can write the energy of the system as

$$E = \sum_{\langle ij \rangle'} V_{ijs_is_j}, \tag{1}$$

where the sum $\sum_{\langle ij \rangle'}$ is restricted to the couples of neighboring sites occupied by particles only. The entire set of all possible couplings $\{V_{ijkl}\}$ is drawn according to an *a priori* probability distribution $g(V)$ and it is *quenched*, whereas the set of the *realized* interactions $\{V_{ijs_is_j}\}$, i.e. the interaction energies directly contributing to a given configuration of particles on the lattice, is distributed according to a different function which at equilibrium it is proved to be [31]

$$p_{eq}(V, T) = \frac{1}{\mathcal{N}(T)} \, g(V) \, e^{-V/k_B T}, \tag{2}$$

where $\mathcal{N}(T)$ is a normalization constant. In the following we adopt natural units, hence $k_B = 1$. Several choices are possible for the *a priori* distribution $g(V)$ and in this work we adopted the same model as in [31], and hence g is a uniform distribution defined on the closed interval $V \in [V_0, V_1]$, with $V_1 = -V_0 = 0.5$. The equilibrium sampling is performed by means of a kinetic Monte Carlo for activated hopping dynamics. Each particle can hop to the position of a neighboring void with a rate

$$w = w_0 \exp\left[-\frac{1}{T}\left(E_0 + \frac{\Delta E}{2}\right)\right], \tag{3}$$

where ΔE is the energy change of the system induced by the hop. We set $w_0 = 10^6$ and $E_0 = 1.5$ so that $E_0 + \Delta E/2 \geq 0$.

RESULTS

In this work we study the relaxation dynamics of the system energy (1), which is akin to the enthalpy relaxation [21, 22]. Following [1] we study the fractional departure from equilibrium defined as the ratio

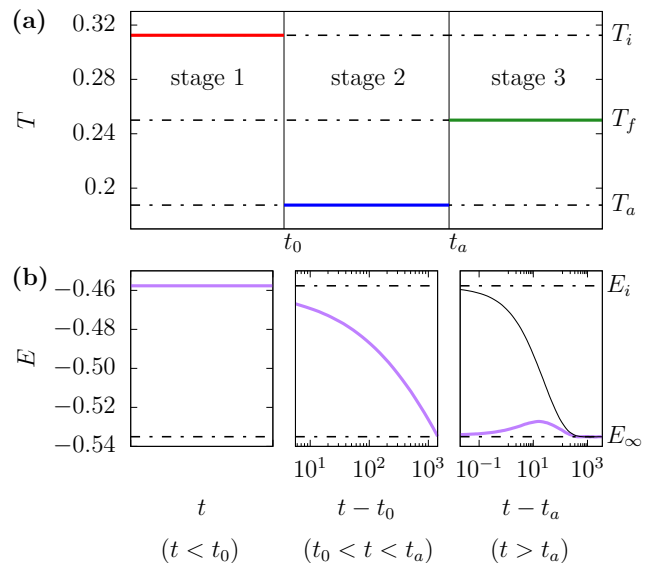$$\delta_E(t) = \frac{E(t) - E_\infty}{|E_\infty|}, \tag{4}$$

FIG. 1: Schematic of the memory protocol: Panels (a) and (b) report the three stages of the protocol for the temperature and energy respectively. Stage 1: The system starts from equilibrium at the initial temperature $T_i = 0.3125$. Stage 2: At time t_0 the temperature jumps to $T_a < T_i$ (down-jump) and the energy relaxes. Stage 3: At time t_a the instantaneous value of the energy equals the equilibrium one at the final temperature T_f, i.e. $E(t_a) = E_\infty$ and the second temperature jump to $T_f > T_a$ (up-jump) is performed. The energy shows a non-monotonic behavior passing trough a maximum and relaxing back to the final equilibrium value. The black solid line reports the energy relaxation after a single down-jump with same T_i and T_f.

where E_∞ is the equilibrium energy at the final temperature T_f and $E(t)$ is the instantaneous value according to (1). Averages have been computed over a thousand independent runs with different initial random seeds. The two-temperatures protocol is somewhat more complicated than the single-jump one, and it is reported for clarity in Fig. 1. The protocol can be divided in three stages: During the first stage, for $t < t_0$, the system is at equilibrium at the initial temperature T_i, with a constant energy E_i (see Fig. 1); the second stage begins at t_0 when the temperature is changed to the annealing value T_a, with $T_a < T_i$ (down-jump), and the energy decreases (see Fig. 1); the third stage begins at t_a when the energy reaches the value $E(t_a) = E_\infty$, i.e. the equilibrium energy at the final temperature T_f, and the temperature is changed once more to the final value T_f, with $T_a < T_f$ (up-jump) and $T_f < T_i$. The hallmark of glassy dynamics in the third stage consists of the non-monotonic evolution of the energy that reaches a maximum, i.e. the *Kovacs hump*, and relaxes back to the same value already attained at t_a, rather than following a steady evolution at the final temperature T_f with an equilibrium value E_∞.

Following [1] we analyze the two-temperatures jump

dynamics for different values of the annealing temperature T_a while keeping constant the initial $T_i = 0.3125$ and final $T_f = 0.25$ values. In Fig. 2 we report the data coming from the final relaxation during the third stage of the protocol. Two features of the Kovacs hump are related to the value of T_a: The peak position and its height. Fig. 2 shows that for lower values of the annealing temperature T_a the peak is higher and it is reached at an earlier time, which agrees with what has been observed in [1]. In the DPLM the equilibrium distribution of the interaction energies is given by Eq. (2) which holds at the end of the relaxation, i.e. it is the long time limit of the instantaneous distribution $p(V,t)$. At the final temperature T_f Eq. (2) yields E_∞ as average energy, i.e. $E_\infty = \sum_{\langle ij \rangle'} \langle V_{ij} s_i s_j \rangle_{T_f}$. Hence, at the end of the annealing stage t_a, the instantaneous probability distribution $p(V,t_a)$ only yields an average value which coincides with that of $p_{eq}(V,T_f)$, but the two distributions are quantitatively different. Hence, the Kovacs hump is due to the further relaxation of the instantaneous distribution $p(V,t)$ towards $p_{eq}(V,T_f)$ for $t > t_a$.

CONCLUSIONS

In the present work we show that the DPLM is able to capture the phenomenology of the Kovacs effect. This is done rather naturally in DPLM without any modification to its original definitions [31]. Important features of Kovacs' non-equilibrium dynamics automatically emerge in the DPLM. It will be interesting to investigate other phenomena where non-equilibrium effects dominate the relaxation behavior of glasses: Ongoing studies of calorimetric spectroscopy reproducing several features of α and β peaks, and of the heat capacity overshoot and hysteresis in time-modulated differential scanning calorimetry, are yielding results consistent with experiments and will be reported elsewhere.

ACKNOWLEDGEMENTS

* Electronic address: C.H.Lam@polyu.edu.hk
† Present Address: Department of Mechanics and Aerospace Engineering, Southern University of Science and Technology, Shenzhen, Guangdong 518055, China
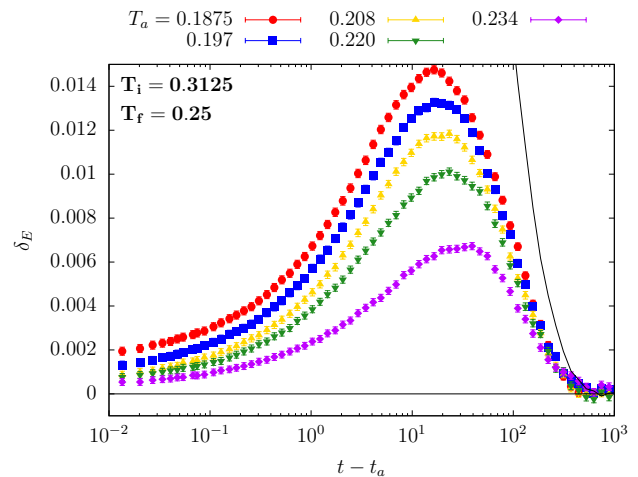

FIG. 2: Dynamics of δ_E for the Kovacs' memory protocol [see Fig.1]. Initial $T_i = 0.3125$ and final $T_f = 0.25$ temperatures are fixed and different annealing temperatures are simulated: The peaks height is the largest and the peak appears the earliest for the lowest annealing temperature $T_a = 0.1875$. The higher T_a the smaller the peak and the later its position. The black solid line reports the energy relaxation after a single down-jump with same T_i and T_f. These features are consistent with what observed in [1].

[1] A. J. Kovacs, in *Fortschritte Der Hochpolymeren-Forschung* (Springer Berlin Heidelberg, Berlin, Heidelberg, 1964) pp. 394–507.
[2] I. M. Hodge, Journal of Non-Crystalline Solids **169**, 211 (1994).
[3] C. A. Angell, K. L. Ngai, G. B. McKenna, P. F. McMillan, and S. W. Martin, Journal of Applied Physics **88**, 3113 (2000).
[4] C. B. Roth, Polymer Glasses , 1 (2016).
[5] G. B. McKenna, Y. Leterrier, and C. R. Schultheisz, Polymer Engineering & Science **35**, 403 (1995).
[6] G. B. McKenna, M. G. Vangel, A. L. Rukhin, S. D. Leigh, B. Lotz, and C. Straupe, Polymer **40**, 5183 (1999).
[7] S. Kolla and S. L. Simon, Polymer **46**, 733 (2005).
[8] T. Hecksher, N. B. Olsen, K. Niss, and J. C. Dyre, The Journal of Chemical Physics **133**, 174514 (2010).
[9] T. Hecksher, N. B. Olsen, and J. C. Dyre, The Journal of Chemical Physics **142**, 241103 (2015).
[10] S. Banik and G. B. McKenna, Phys. Rev. E **97**, 062601 (2018).
[11] L. C. Struik, Polymer **38**, 4677 (1997).
[12] L. C. Struik, Polymer **38**, 5233 (1997).
[13] L. Berthier and J.-P. Bouchaud, Phys. Rev. B **66**, 054404 (2002).
[14] E. M. Bertin, J.-P. Bouchaud, J.-M. Drouffe, and C. Godrche, Journal of Physics A: Mathematical and General **36**, 10701 (2003).
[15] L. F. Cugliandolo, G. Lozano, and H. Lozza, The European Physical Journal B - Condensed Matter and Complex Systems **41**, 87 (2004).
[16] S. Mossa and F. Sciortino, Phys. Rev. Lett. **92**, 045504 (2004).
[17] A. Buhot, Journal of Physics A: Mathematical and General **36**, 12367 (2003).

[18] J. J. Arenzon and M. Sellitto, The European Physical Journal B - Condensed Matter and Complex Systems **42**, 543 (2004).

[19] G. Aquino, A. Allahverdyan, and T. M. Nieuwenhuizen, Phys. Rev. Lett. **101**, 015901 (2008).

[20] A. Prados and J. J. Brey, Journal of Statistical Mechanics: Theory and Experiment **2010**, P02009 (2010).

[21] S. Montserrat, Journal of Polymer Science Part B: Polymer Physics **32**, 509 (1994).

[22] L. Grassia, Y. P. Koh, M. Rosa, and S. L. Simon, Macromolecules **51**, 1549 (2018).

[23] F. Krzakala and F. Ricci-Tersenghi, Journal of Physics: Conference Series **40**, 42 (2006).

[24] L. Berthier and P. C. W. Holdsworth, EPL (Europhysics Letters) **58**, 35 (2002).

[25] A. Q. Tool, Journal of the American Ceramic Society **29**, 240 (1946).

[26] O. S. Narayanaswamy, Journal of the American Ceramic Society **54**, 491 (1971).

[27] C. T. Moynihan, P. B. Macedo, C. J. Montrose, C. J. Montrose, P. K. Gupta, M. A. DeBolt, J. F. Dill, B. E. Dom, P. W. Drake, A. J. Easteal, P. B. Elterman, R. P. Moeller, H. Sasabe, and J. A. Wilder, Annals of the New York Academy of Sciences **279**, 15 (1976).

[28] A. J. Kovacs, J. J. Aklonis, J. M. Hutchinson, and A. R. Ramos, Journal of Polymer Science: Polymer Physics Edition **17**, 1097 (1979).

[29] R. E. Robertson, R. Simha, and J. G. Curro, Macromolecules **17**, 911 (1984).

[30] G. A. Medvedev and J. M. Caruthers, Macromolecules **48**, 788 (2015).

[31] L.-H. Zhang and C.-H. Lam, Phys. Rev. B **95**, 184202 (2017).

[32] C.-S. Lee, M. Lulli, L.-H. Zhang, H.-Y. Deng, and C.-H. Lam, arXiv e-prints , arXiv:1909.03240 (2019), arXiv:1909.03240 [cond-mat.soft] .

[33] M. Lulli, C.-S. Lee, H.-Y. Deng, C.-T. Yip, and C.-H. Lam, arXiv e-prints , arXiv:1909.03685 (2019), arXiv:1909.03685 [cond-mat.soft] .

[34] C.-H. Lam, Journal of Statistical Mechanics: Theory and Experiment **2018**, 023301 (2018).

[35] H.-Y. Deng, C.-S. Lee, M. Lulli, L.-H. Zhang, and C.-H. Lam, Journal of Statistical Mechanics: Theory and Experiment **2019**, 094014 (2019).